Hydrological Application of Land Surface Backscattering Coefficients Observed by Low-resolution Radars from Space

Shinta Seto[1], Taikan Oki[1] and Katumi Musiake[1]
[1]*Institute of Industrial Science, University of Tokyo, Meguro-ku, Tokyo, 153-8505, Japan*

ABSTRACT: The potential of active 'low-resolution' microwave sensors for soil moisture monitoring has been analyzed. These sensors can observe land surface at multiple incident angles (not simultaneously). By sensitivity analysis considering mosaic of land cover, it is assumed that smaller incident angle is better for soil moisture monitoring. The back scattering coefficients data observed by ERS/WSC (windscatterometer) are analyzed with soil moisture data calculated by water and energy balance model at land surface. The data analysis also shows that smaller incident angle is suitable for soil moisture monitoring.

1 INTRODUCTION

Radars have been developed and operated mainly for the rainfall observation, but some of them can be applied for the land surface monitoring. Radars on satellite can measure the land surface backscattering coefficients, from which information about soil moisture and/or vegetation density can be inferred. Some of the satellite-borne radars have high spatial resolution of about 10 meters owing to the synthetic aperture technique. Synthetic Aperture Radars (SARs) have been board on such satellites as JERS, ERS, and RADARSAT. Their high spatial resolution is effective for monitoring the land surface in detail. However, the frequency of observation by these high-resolution sensors is once per more than one month. More frequent observation is desired for some hydrological applications.

The backscattering coefficients observed by the low-resolution sensors are expected to reflect the large-scale information of land surface. In this study, the land surface backscattering coefficients data are analyzed to examine how the backscattering coefficients are reflected with the land surface status.

2 EFFECTS OF SOIL MOISTURE ON ATMOSPHERE

Soil moisture plays an important role in land-atmosphere interaction, especially in continental scales. Shukla and Mintz (1982) showed that soil moisture affects seasonal prediction of precipitation in their GCM simulation. However, the direct observation of soil moisture is very scarce in the world. Remote sensing technique is a unique way to observe soil moisture in large scale.

3 SENSORS AND DATA

Sensors with low-spatial resolution can observe the land surface with high-temporal frequency. The European Remote-sensing Satellite (ERS)-1,2 have windscatterometers (ERS/WSC), whose spatial resolution is 50km. Another example is the Precipitation Radar (PR) board on the Tropical Rainfall Measuring Mission (TRMM). TRMM/PR is the first precipitation radar on satellites and it can measure the vertical structure of rainfall in tropics (within 37 N and 37 S). TRMM/PR observes the land surface and the rainfall simultaneously.

These low-spatial resolution sensors can observe by multiple incident angles (not simultaneously), while the incident angle of SAR is almost fixed. The incident angle of ERS/WSC is 17degrees to 57degrees, and that of TRMM/PR is 0 degrees to 18 degrees.

4 ANNUAL AVERAGE

The spatial distribution of backscattering coefficients corresponds with land cover, or vegetation. The annual average of the backscattering coefficients observed by two sensors at different incident angles are shown in Figure 1 and Figure 2. Figure 3 shows the average backscattering coefficients observed by different land cover types. The backscattering coefficients observed at desert shows strong dependence on incident angle, while the backscattering coefficients observed at forest shows weak dependence on incident angle. It is surprising that the backscattering coefficients observed by two sensors is almost same around 20 degrees of incident angle.

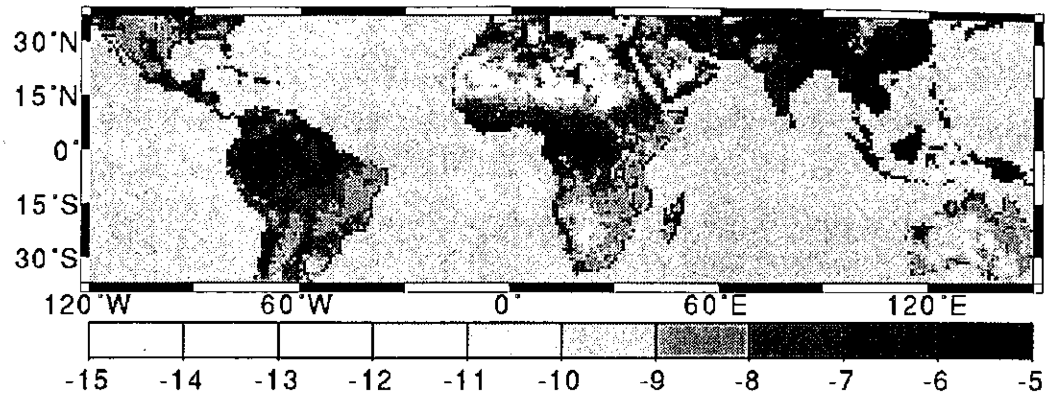

Figure 1. Global maps of annual average of the backscattering coefficients observed by ERS/WSC (incident angle is 20 degree)

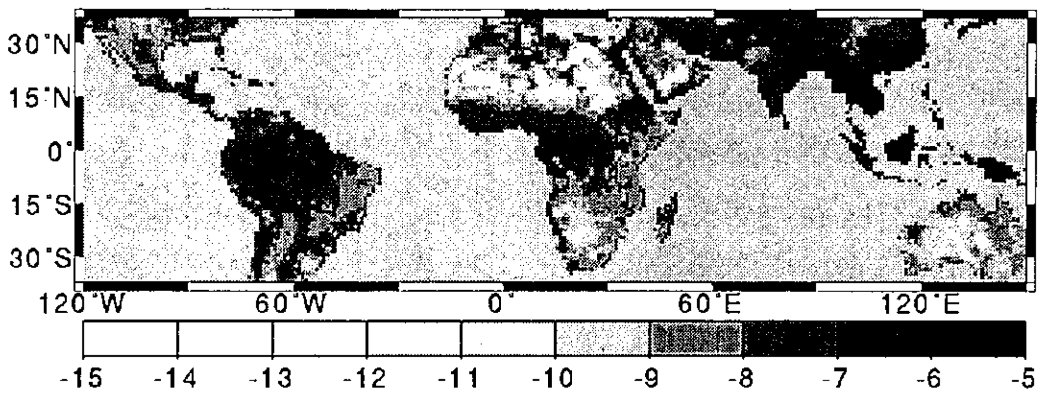

Figure 2. Global maps of annual average of the backscattering coefficients observed by TRMM/PR (incident angle is 18 degree)

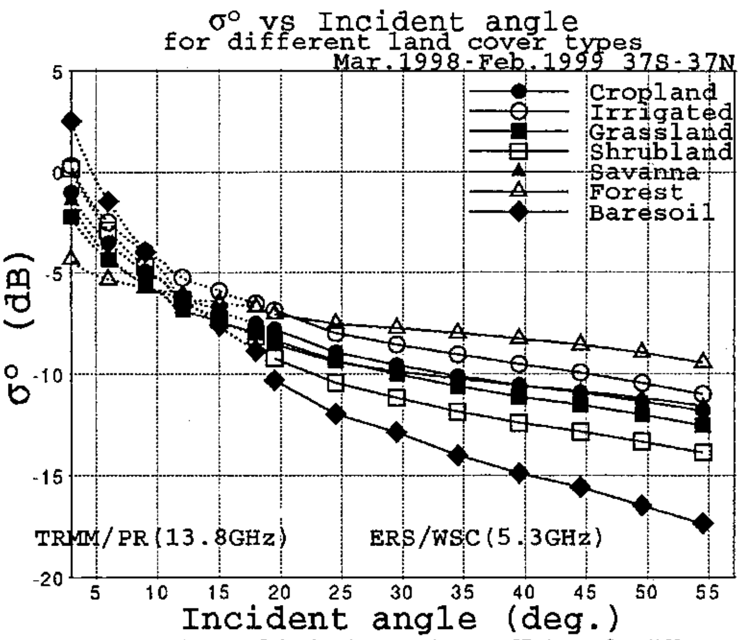

Figure 3. Incident angle dependence of the backscattering coefficients for different land cover types.

5 HETEROGENITY OF LAND SURFACE AND TENTATIVE MODELLING

A simple model to explain the backscattering coefficients of low-spatial resolution sensors is proposed as Eq. (1).

$$\sigma^0 = (1-f)\sigma_s^0(Mv) + f\sigma_v^0 \tag{1}$$

where σ^0 is total backscattering coefficients, f is the fraction of vegetation cover, σ_s^0 is the backscattering coefficients from soil (non-vegetated) surface, σ_v^0 is the backscattering coefficients from vegetated surface. Penetration into vegetation is ignored here. Only σ_s^0 is affected by soil moisture and following relationship is used here.

$$\sigma_s^0(Mv)(dB) = \sigma_s^0(Mv=0\%)(dB) + c \times Mv \tag{2}$$

where c is constant. In this formulation, we consider the mosaic within observation area. As ERS/WSC or TRMM/PR has lower resolution than SAR sensors, it seems to be important to consider the mosaic of land cover types. In desert, f is assumed to be nearly zero and in forest, f is assumed to be nearly one. Therefore, σ_s^0 and σ_v^0 can be approximated to σ^0 of bare soil and σ^0 of forest respectively.

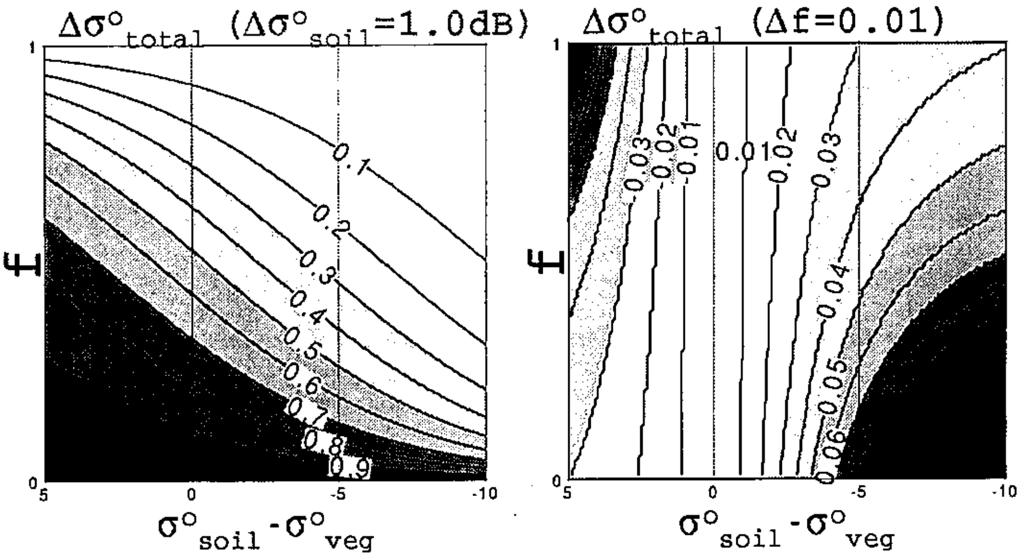

Figure 4. Sensitivity of σ^0 derived by tentative theory. (a) to soil moisture. (b) to NDVI.

To study the sensitivity of σ^0 to soil moisture or vegetation, Eq. (1) is differentiated by Mv or f as Eq. (3) and Eq. (4), respectively.

$$\frac{\partial \sigma^0(dB)}{\partial Mv} = \frac{(1-f)10^{b/10}}{(1-f)10^{b/10} + f} \cdot c \tag{3}$$

$$\frac{\partial \sigma^0}{\partial f} = \frac{-10^{b/10}+1}{(1-f)10^{b/10} + f} \tag{4}$$

where $b = \sigma_s^0(dB) - \sigma_v^0(dB)$. Figure 4 is contour maps of the increase of σ^0 when σ_s^0 increases 1(dB) and *f* increases 0.01 respectively. Horizontal axis is set to the parameter *b* and vertical axis is set to the parameter *f*. We can see from these figures that the sensitivity of σ^0 to soil moisture is high when the parameter *b* is high. As Figure 3 shows, the parameter *b* is higher when the incident angle is small. Therefore, the sensitivity to soil moisture is higher when the incident angle is small. On the other hand, the sensitivity of σ^0 to the parameter *f* (fraction of vegetation) is higher when the incident angle is large. When the incident angle is 12 degrees, the parameter *b* is almost zero. At this incident angle, σ^0 is almost independent from the parameter *f* (fraction of vegetation). These figures also indicate that the sensitivity is less when the parameter *f* is large (the vegetation cover is dense).

6 DATA ANALYSIS

The sensitivity of σ^0 observed by different incident angles to soil moisture is analyzed by ERS/WSC data. Here, the soil moisture calculated by Nijssen et al. (2001) and the NDVI data provided as NOAA/AVHRR GAC data are used for data analysis. Due to limitation of data length, the analysis is done for January of 1992 through December of 1993. All data are gridded into 2 degrees by 2 degrees. The temporal resolution is monthly.

The simultaneous correlation coefficients between σ^0 and soil moisture (RS) and the simulatanesous correlation coefficients between σ^0 and NDVI (RN) are calculated. As the number of data is 24, the correlation coefficients more than 0.52 is judged as significantly positive correlated (significance level is 1%). Each grid was classified into 5 types based on the correlation coefficients. (a) only RS is statistically significant (denoted as SS, later on). (b) only RN is statistically significant (denoted as SN) (c) Both RS and RN are statistically significant, but RS is larger than RN (denoted as WS) (d) Both RS and RN are statistically significant, but RN is larger than RS (denoted as WN). (e) Neither RS nor RN is statistically significant (denoted as NC).

The classification results are shown in Figure 5 (in case of 20 degrees and 55 degrees). In case of 20 degrees, more grids are classified as SS or WS. In case of 55 degrees, more grids are classified as SN or WN. Deserts (like Sahara) and dense forests (like Amazon, Congo) are classified as NC. The number of grids classified as SS, WS, SN, WN, NC are shown as histogram in Figure 6. We can see that the number of grids classified as SS or WS decreases and the number of grids classified as SN or WN increases as incident angle is larger. As of the sensitivity analysis, σ^0 observed by smaller incident angle is more affected by soil moisture.

Figure 7 shows the time series of σ^0, soil moisture, and NDVI. In the region around India (75-80E, 20-25N), σ^0 corresponds with soil moisture rather than NDVI. σ^0 reaches the peak in August of 1992, soil moisture also reaches the peak in August, but NDVI does in September. In the Sahel of Africa (15-20E, 10-15N), σ^0 corresponds with NDVI rather than soil moisture. This difference between these two regions indicates that in the Sahel of Africa, the seasonal change of *f* is strong compared with other regions. Siberia also shows similar results as the Sahel of Africa.

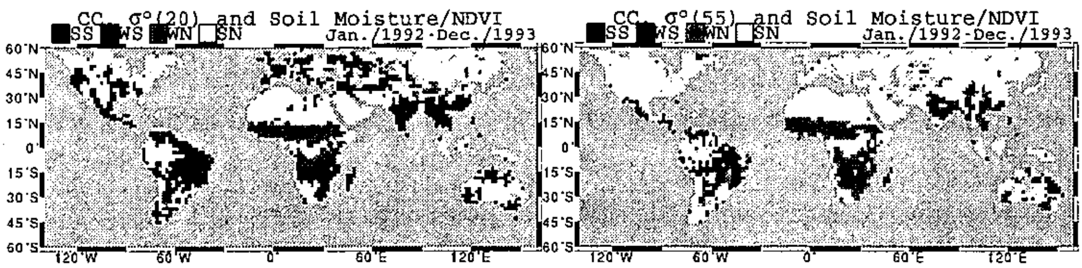

Figure 5. The classification based on correlation coefficients between σ^0 and soil moisture/NDVI. (a) in case of 20 degrees. (b) in case of 55 degrees.

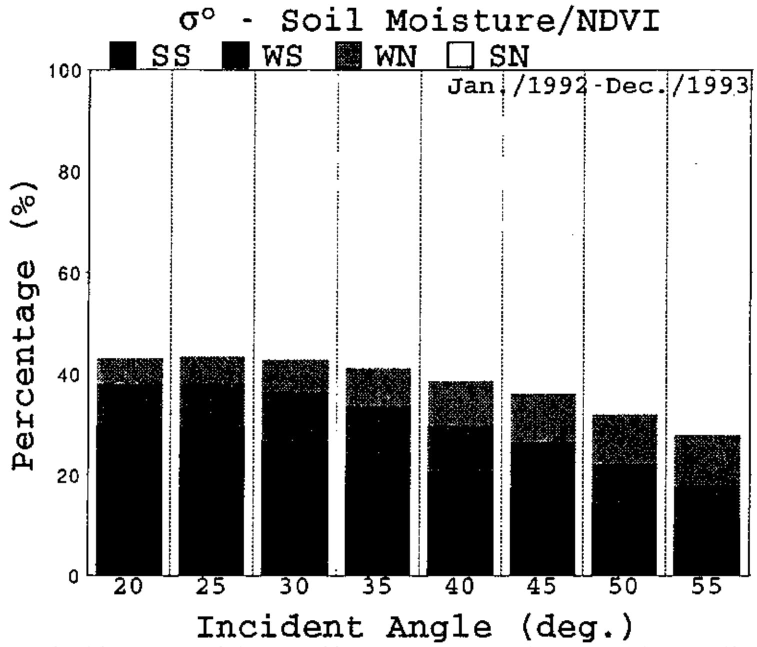

Figure 6. The histogram of the classification based on the correlation coefficients.

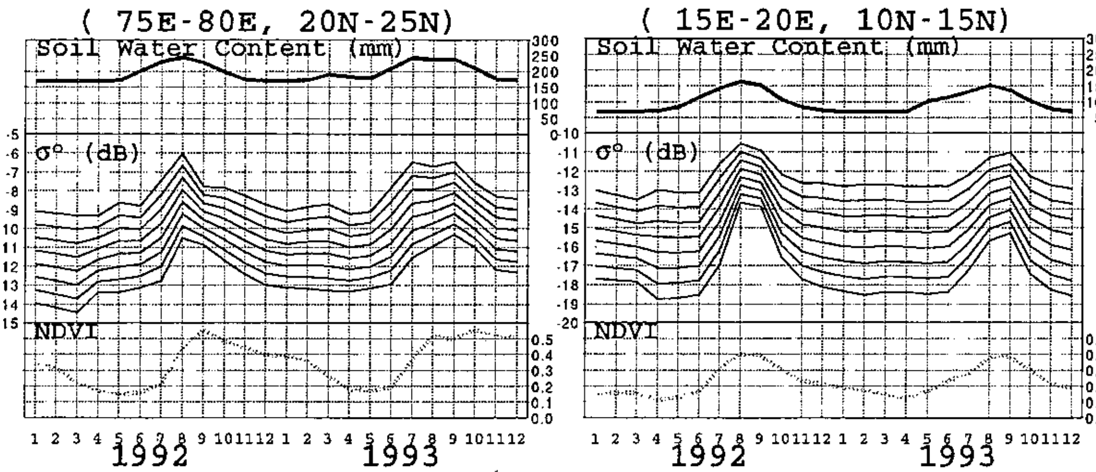

Figure 7. The time series of σ^0, soil moisture, and NDVI. (a)the region around India (75-80E, 20-25N). (b) the region around the Sahel of Africa (20-25E, 10-15N).

Sensitivity of σ^0 to soil moisture or NDVI is calculated by data as follows. To calculate the sensitivity to soil moisture, grids which are classified as SS at every incident angle are selected. To calculate the sensitivity to NDVI, grids which are classified as SN at every incident angle are selected. These selections are to avoid the effect of each other (NDVI or soil moisture) on σ^0 as much as possible. Sensitivity is calculated by regression analysis.

Results are shown as contour maps in Figure 8. The horizontal axis is set to be incident angle and the vertical axis is set to be annual average of NDVI. The pattern of contour maps in Figure 4 and Figure 8 is qualitatively similar. If NDVI is smaller, the sensitivity is larger. In Figure 8, the sensitivity is maximum in case the annual average of NDVI is 0.2 – 0.3. Where the annual average of NDVI is 0.1, the sensitivity is shown to be small. In such area, the change of soil moisture is small and regression analysis is not so reliable. The sensitivity to soil moisture decreases at larger incident angles, but it does not decrease so much compared with Figure 4. On the other hand, the sensitivity to NDVI increases at larger incident angles. This suggests the reason why σ^0 is less affected by soil moisture at larger incident angles. The sensitivity to soil moisture itself is not so small at larger incident angles, but the sensitivity to NDVI is large at larger incident angle. The effect of seasonal change of

NDVI on σ^0 masks the effect of soil moisture on σ^0. If this reason is true, by removing the effect of seasonal change of NDVI, the data observed at larger incident angles can be used for soil moisture estimation. In Sahel or Siberia, where the seasonal change of NDVI seems to be strong, such technique is needed even if we use σ^0 observed by smaller incident angles.

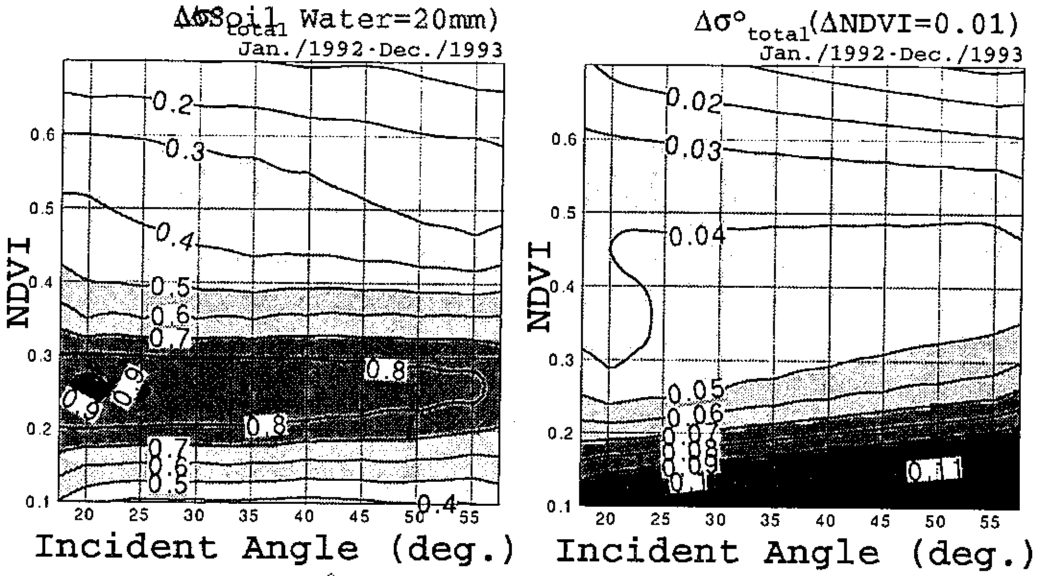

Figure 8. Sensitivity of σ^0 derived by data analysis. (a) to soil moisture. (b) to NDVI.

7 CONCLUSION

The seasonal change of σ^0 observed by active 'low-resolution' microwave sensors is shown to have potential for soil moisture retrieval. Such sensors can observe by multi incident angles. It is found by data analysis that smaller incident angle is more suitable for soil moisture retrieval. σ^0 observed by larger incident angles corresponds with NDVI rather than with soil moisture. This may be not because the sensitivity to soil moisture is weak, but because the sensitivity to NDVI is strong. The technique to minimize the effect of NDVI on σ^0 should be developed. That makes the potential of active 'low-resolution' sensors for soil moisture estimation higher.

8 REFERENCES

Nijssen, B., R. Schnur, D.P. Lettenmaier (2001). "Global Retrospective Estimation of Soil Moisture Using the Variable Infiltration Capacity Land Surface Model 1980-93", Journal of Climate, 14, 1790-1808.

Shukla, J. and Y. Mintz (1982). "Influence of land-surface Evapotranspiration on the earth's climate", Science, 215, 1498-1501.

Wismann, V., A (1999). "Database of Global C-band NRCS derived from ERS scatterometer data", IEEE Geoscience and Remote Sensing Newsletter, 106, 7-9.